Magnetic circular dichroism and optically detected electron paramagnetic resonance of trapped hole centres in KBr and KI

1994 J. Phys.: Condens. Matter 6 1801

(http://iopscience.iop.org/0953-8984/6/9/021)

J. Phys.: Condens. Matter 6 (1994) 1801–1814. Printed in the UK

Magnetic circular dichroism and optically detected electron paramagnetic resonance of trapped hole centres in KBr and KI

J M Spaeth†, W Meise† and K S Song‡

† Fachbereich Physik, Universität-GH Paderborn, Warburger Strasse 100, D-33098 Paderborn, Germany

‡ Department of Physics, University of Ottawa, Ottawa, Ontario, Canada K1N 6N5

Received 9 November 1993

Abstract. In KBr and KI the magnetic circular dichroism of the optical absorption (MCDA) of V_K and H centres created by x-irradiation at 4.2 K *in situ* was investigated as well as the MCDA-detected electron paramagnetic resonance (EPR) spectra. MCDA extrema were found at the spectral positions of the known absorption band peaks for V_K centres including a second band in the ultraviolet (UV), which had been reported previously for KI but not for KBr. Only one MCDA band was found for H centres, corresponding to the infrared (IR) transition. No MCDA-detected EPR spectra were observed for V_K and H centres with their molecular axes parallel to the magnetic field. Using perturbation theory to describe the effect of spin–orbit coupling and magnetic field mixing of the X_2^- molecular orbitals used to describe V_K and H centres previously, the experimental results could be explained except for the new UV MCDA band, which cannot be explained assuming inversion symmetry of the V_K centres. It is suggested that this band arises because of the low-frequency (10^{12} s^{-1}) axial displacement mode of V_K centres, breaking the inversion symmetry, which is a quasi-static distortion for the optical transition, but fast with respect to EPR, and therefore not seen there.

1. Introduction

Trapped hole centres have been investigated intensively in the alkali halides with optical spectroscopy and electron paramagnetic resonance (EPR) (Schoemaker 1973, Itoh 1972, Cade *et al* 1984, Fowler 1968). They are known as H centres and V_K centres, respectively. H centres consist of a $halogen_2^-$ molecular ion on a halogen lattice site, whereas in V_K centres a hole is shared between two adjacent halogen ions along (110) directions (figure 1). H centres are found as a result of the decay of self-trapped excitons (Song and Williams 1993), whereby F centres are formed simultaneously (electron trapped in a halogen vacancy). For the formation of V_K centres it is necessary for an electron trap to be present in the crystal. V_K and H centres are created by ionizing radiation and are only stable below room temperature.

Trapped hole centres play a fundamental role in the luminescence processes in ionic crystals such as exciton decay luminescence or recombination processes between trapped electron and trapped hole centres. They are of key importance in all scintillator crystals for the detection of x-ray radiation. In particular, in the application of scintillator crystals for computer tomography it turned out that trapped hole centres play a detrimental role by causing after-glow effects, which was demonstrated recently in the well known system CsI:Tl (Spaeth *et al* 1993, Meise 1993).

0953-8984/94/091801+14$19.50

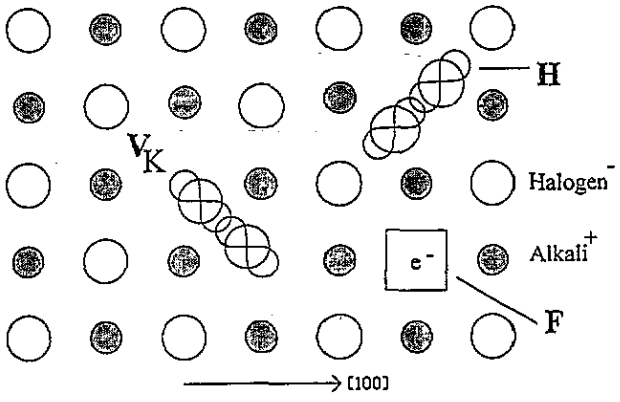

Figure 1. Models of V_K, H and F centres in a cubic alkali halide.

In the well known X-ray storage phosphor BaFBr:Eu trapped hole centres play a decisive role in the information storage, which is not yet understood at all (Eachus *et al* 1991a, b, Koschnick *et al* 1992a, b). Both in the case of the after-glow effect in scintillator crystals and in the case of the storage phosphors the concentration of hole centres is too small to be detected by conventional EPR. Therefore more sensitive methods such as optically detected EPR (ODEPR) must be used for their investigation. Such investigations had not yet been performed on trapped hole centres.

In this paper we report on ODEPR investigations of H and V_K centres in KBr and KI using the magnetic circular dichroism of the absorption (MCDA) (for details see e.g. Spaeth *et al* 1992). It turned out that it was not straightforward to understand either the MCDA bands or the EPR spectra with the theoretical model for the centres discussed so far. We report on new optical transitions of both centres discovered via the MCDA as well as upon an improved theoretical model to understand the magneto-optical properties of H and V_K centres.

2. Experiment

Extremely pure KBr and KI crystals especially prepared for the investigation of H centres were used. The KBr crystal was provided by W G McDugle (Eastman Kodak Corporation). The highly pure KI was grown at the crystal growth laboratory of the University of Paderborn. To study V_K centres the KBr and KI crystals were doped with Tl (approximately 0.5 mol% in the melt). The samples were cleaved and oriented perpendicular to (100) faces. The MCDA and ODEPR spectra were measured with a custom-built computer-controlled spectrometer working in the K band (24 GHz) between 1.5 K and room temperature in the spectral range from 220 nm to 1.7 μm. The samples could be x-irradiated (70 kV, 15 mA) *in situ* in the cavity at all temperatures.

3. Experimental results

3.1. Absorption and MCDA spectra

Figure 2(*b*) shows the MCDA spectrum of KBr x-irradiated at 4.2 K and figure 2(*a*) the absorption bands of V_K and H centres taken from the literature (Fowler 1968, Delbecq *et al* 1961). The MCDA is the differential absorption of right and left circularly polarized light

measured in a longitudinal static magnetic field. When KBr is not extremely pure V_K and H centres are produced, together with F centres. In the MCDA spectrum the dominant band is that of F centres with a derivative-like structure at about 2.06 eV. The three extrema at 3.2 eV, 1.65 eV and 1.4 eV correlate with the peaks of the absorption bands of the V_K centres. A further extremum at 2.8 eV cannot be correlated with any known absorption band. It originates in a paramagnetic ground state, since it is magnetic field and temperature dependent (see e.g. Spaeth *et al* 1992). Had the V_K centre an MCDA with a derivative-like structure like that of the F centres, one would expect the passing through zero to happen at 3.2 eV and not at 3.0 eV.

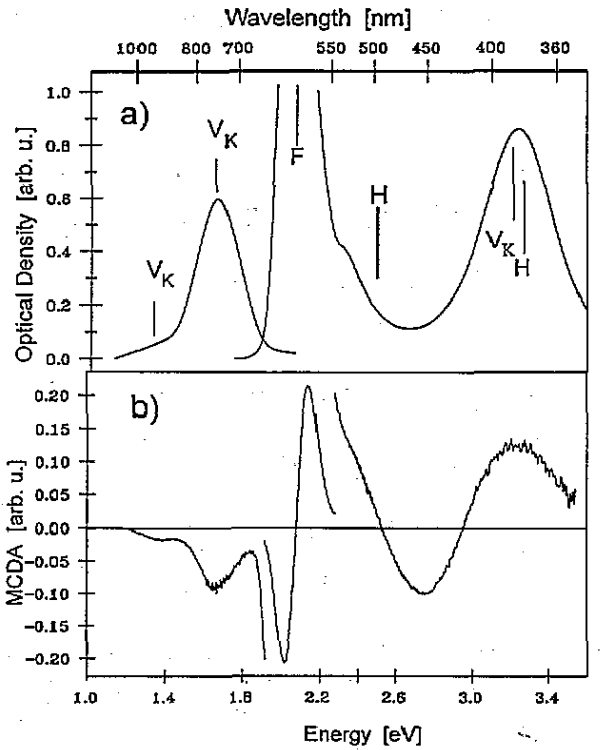

Figure 2. (*a*) Absorption bands of V_K, H, and F centres in KBr, generated by x-irradiation below 20 K. (*b*) MCDA spectrum of KBr x-irradiated at 4.2 K *in situ*, measured at 1.5 K; magnetic field, 2 T.

No MCDA band can be clearly assigned to H centres. Note, however, that the known bands at 3.3 eV and at 2.5 eV are superimposed by the strong signals from V_K and F centres respectively.

Similar results were obtained for KI. Curve 1 in figure 3(*b*) is measured for an undoped KI crystal, curve 2 for a Tl-doped crystal. The MCDA band at 2.23 eV can be correlated with one of the known H-centre absorption bands at 2.23 eV and 2.78 eV (Konitzer and Hersh 1966). The behaviour of the 2.23 eV MCDA is exactly that of the absorption band: upon warming the crystal to 70 K it is red-shifted to 2.15 eV because of the formation of H_A centres (Konitzer and Hersch 1966). In the Tl-doped crystal (figure 3(*b*), curve 2) the V_K centre bands dominate. The MCDA bands at 1.1 eV and at 1.55 eV correlate with the

known absorption bands (Delbecq *et al* 1961). A significant MCDA at 3.1 eV, expected from the optical absorption, is not observed, but rather two bands at 2.1 eV and 2.8 eV. Again, it was not possible to clearly separate the MCDA bands of V_K and H centres in the MCDA spectra in KI either.

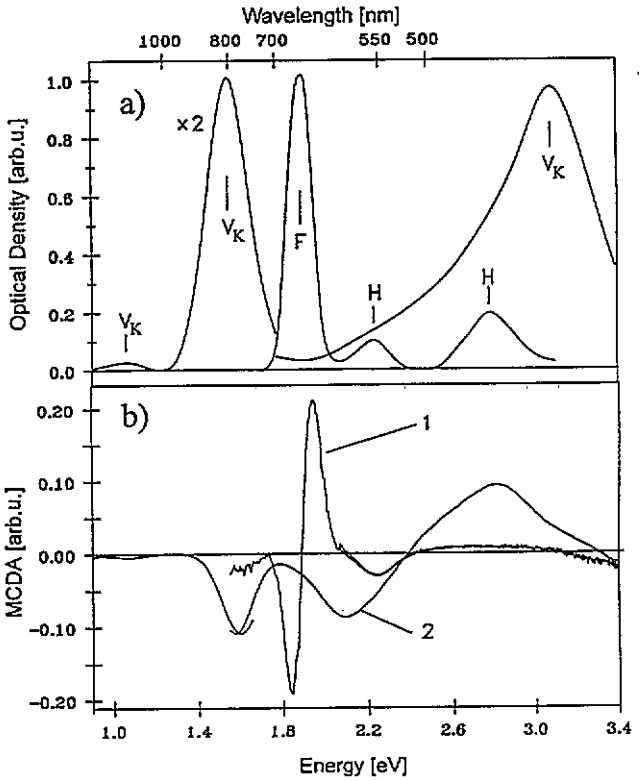

Figure 3. (*a*) Absorption bands of V_K, H, and F centres in KI, generated by x-irradiation below 20 K. (*b*) MCDA spectrum of KI, x-irradiated at 4.2 K *in situ*, measured at 1.5 K; magnetic field, 2 T. Curve 1, undoped KI; curve 2, Tl-doped KI (doping level 0.5 mol% in the melt).

3.2. ODEPR

Figure 4 shows various measurements of the ODEPR of a 'pure' KBr crystal when x-irradiated at 4.2 K. The ODEPR signals are microwave-induced changes (diminutions) of the MCDA (Spaeth *et al* 1992). Figure 4, traces b and d, show the ODEPR measured in the infrared (IR) V_K MCDA band at 1.65 eV for $\boldsymbol{B}_0 \parallel [100]$ and [110], respectively. For $\boldsymbol{B}_0 \parallel [100]$ there are V_K centres, the axes of which are either perpendicular to $\boldsymbol{B}_0$ or at angles of 45°. If $\boldsymbol{B}_0 \parallel [110]$ one has V_K centres with orientations of 0°, 90° and 60° with respect to the static magnetic field. For the EPR spectra of V_K centres one expects to measure the typical seven-line hyperfine (HF) pattern because of the two equivalent Br nuclei with $I = \frac{3}{2}$ with the intensity ratio of 1:2:3:4:3:2:1. In figure 4 the expected spectra from the known EPR parameters ($g_\parallel$, $g_\perp$, $A_\parallel$ and $A_\perp$: $g_{\parallel,\perp}$ being the g-factors, $A_{\parallel,\perp}$, the HF interaction constants) are indicated by bars for the various centre orientations, that of 90° with a simulation of the

spectrum. Note that due to the rather large line widths often found in ODEPR (Spaeth *et al* 1992) the small differences in the HF interactions of the two isotopes ^{79}Br and ^{81}Br are not resolved (^{79}Br, $I = \frac{3}{2}$, 50.7% abundance, $g_I = 1.404\,266$; ^{81}Br, $I = \frac{3}{2}$, 49.3% abundance, $g_I = 1.513\,706$). It is apparent from figure 4 that no parallel centres were measured, only those at 60°, 45° and 90°, where the latter show the strongest signals. The spin lattice relaxation time T_1 could be measured at 1.6 K to be $T_1 = (1.6 \pm 0.1)$ s.

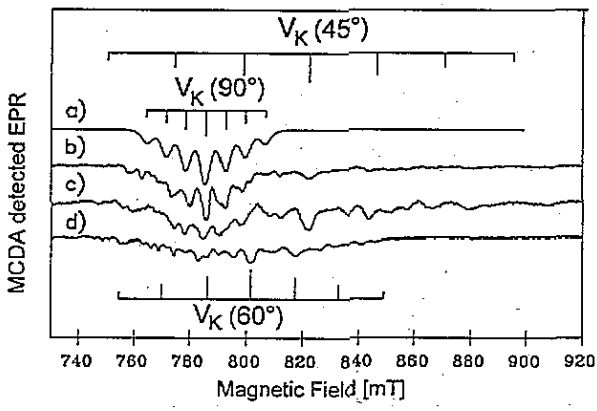

Figure 4. ODEPR spectra of KBr x-irradiated at 4.2 K *in situ*, measured at 1.5 K; microwave frequency, 23.8 GHz. Trace a, calculated EPR spectrum of V_K centres with their axes perpendicular to B_0 with $A_\perp = 7.67$ mT, $g_\perp = 2.162$, and assuming a half width of the hyperfine lines of 3 mT; trace b, measured at a photon energy of 1.65 eV, $B_0 \parallel [100]$; trace c, measured at a photon energy of 2.7 eV, $B_0 \parallel [100]$; trace d, measured at a photon energy of 1.65 eV, $B_0 \parallel [110]$.

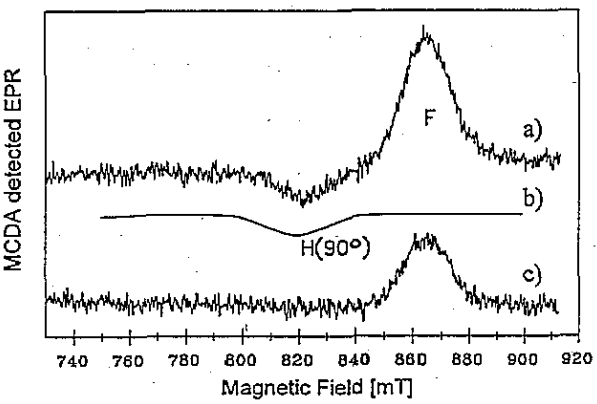

Figure 5. ODEPR spectra of KBr x-irradiated at 4.2 K *in situ*, measured at 1.5 K; microwave frequency, 23.8 GHz. Trace a, measured at a photon energy of 2.4 eV, $B_0 \parallel [100]$; trace b, calculated EPR spectrum of H centres with their axes perpendicular to B_0, with $A_\perp = 5$ mT, $g_\perp = 2.074$, and assuming a half width of the HF lines of 5 mT; trace c, as trace a after annealing to 70 K.

The identification of an EPR spectrum of H centres turned out to be more difficult because of the overlap of the MCDA bands with those of V_K and F centres. Figure 5 shows the ODEPR spectrum (trace a) in KBr measured at 2.4 eV for $B \parallel [100]$ in the spectral region of the known H-centre absorption (Faraday and Compton 1965). The photon energy for the measurement was chosen to be as far away as possible from the V_K absorption band. The EPR line at 870 mT is due to F centres measured because of the overlap of the F- and H-centre MCDA bands at 2.4 eV. The negative signal at about 820 mT is assigned to perpendicular H centres for the following reasons:

(i) the signal vanishes upon warming to 70 K (figure 5, trace c), the temperature where H centres are thermally destroyed;

(ii) the g-factor coincides with that known from the literature (Konitzer and Hersh 1966) for perpendicular centres; and

(iii) the width of the spectrum agrees with that of the EPR of perpendicular H centres.

In conventional EPR $A_\perp$ could not be determined, only the fact that $A_\perp \ll A_\parallel$. The solid line in figure 5, trace b, is a simulation with the known value of $g_\perp$ and the assumption that $A_\perp = 5$ mT. We could not resolve any HF structure, largely because of saturation effects. In the MCDA technique EPR can only be seen for saturating transitions (see e.g. Spaeth *et al* 1992). The assignment of the negative EPR line at 820 mT to H centres will be further supported by measurments of the MCDA tagged by EPR (see below). The spectrum is clearly different from that of the perpendicular V_K centres. As in the case of V_K centres, no parallel centres were observed in ODEPR.

The results for V_K centres in KI are very similar to those found in KBr. Figure 6 shows the ODEPR spectra recorded in a KI crystal doped with Tl and x-irradiated at 4.2 K. V_K centres in KI have a 11-line HF structure because $I(^{127}I) = \frac{5}{2}$ with an intensity ratio of 1:2:3:4:5:6:5:4:3:2:1. As found for KBr, the spectrum for perpendicular centres appears with the largest intensity, while no spectrum was found for parallel centres. The calculated EPR spectrum in figure 6, trace a, was obtained using literature values for $g_\perp$ and the HF interaction parameters (Schoemaker 1973).

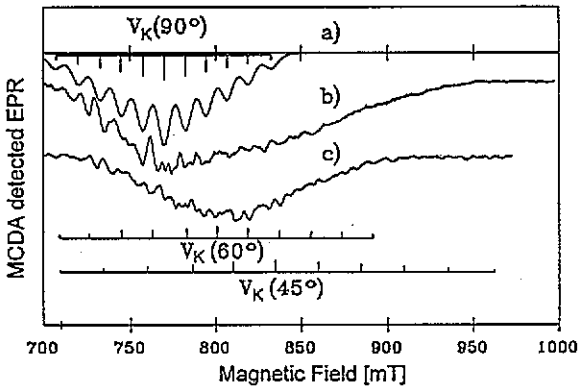

Figure 6. ODEPR spectra of KI x-irradiated at 4.2 K *in situ*, measured at 1.5 K; microwave frequency, 24.5 GHz. Trace a, calculated EPR simulation of V_K centres with their axes perpendicular to B_0, with $A_\perp = 14$ mT, $g_\perp = 2.278$, and assuming a half width of the HF lines of 7 mT; trace b, measured at a photon energy of 2.1 eV, $B_0 \parallel [100]$; trace c, measured at a photon energy of 2.1 eV, $B_0 \parallel [110]$.

In order to study H centres, a particularly pure KI crystal was x-irradiated for several hours at 4.2 K. Figure 7, trace b, shows the ODEPR spectrum measured at 2.25 eV. The extremum found at 2.25 eV corresponds to the H-centre absorption peak known from the literature; it is clearly different from what was found from the V_K centres and F centres. Again, the EPR spectrum peaking at 840 mT is assigned to H centres with the axes perpendicular to the magnetic field orientation. The $g_\perp$ factor was determined to be $g_\perp = 2.08 \pm 0.01$. These are the first EPR data on H centres in KI. The spectrum can be simulated by assuming $A_\perp = 7$ mT and a half width for each HF line of 5 mT. The spin lattice relaxation times of both V_K and H centres are shorter than 0.5 s at $T = 1.5$ K.

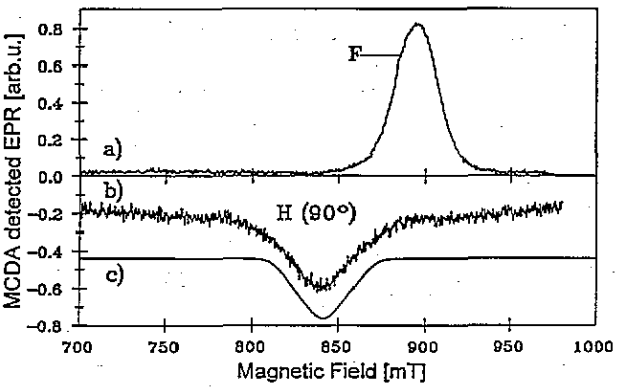

Figure 7. ODEPR spectra of KI x-irradiated at 4.2 K *in situ*, measured at 1.5 K; microwave frequency, 24.5 GHz. Trace a, ODEPR spectrum of F centres, measured at a photon energy of 1.95 eV; trace b, ODEPR of H centres, measured at a photon energy of 2.25 eV, $B_0 \parallel [100]$; trace c, calculated EPR spectrum of H centres with their axes perpendicular to B_0, $A_\perp = 7$ mT, $g_\perp = 2.08$, assuming a half width of HF lines of 5 mT.

3.3. Excitation spectra of the ODEPR

Figure 8(*b*) shows the MCDA spectra 'tagged' by the EPR lines of V_K centres for centres oriented perpendicularly (measured at 787 mT) and oriented at 45° (measured at 823 mT) with respect to the magnetic field and for perpendicular H centres in KBr (measured at 820 mT) in comparison to the total MCDA (figure 8(*a*)). It is seen that V_K centres have an MCDA extremum at 2.7 eV besides the known UV transition at 3.22 eV and in the IR region two extrema at 1.65 and 1.4 eV, respectively, the latter two correlating well with the two known IR bands (figure 8(*a*)). Note that the sign of the transition at 1.4 eV is different for V_K centres with perpendicular orientation and with 45° orientation. H centres have a tagged MCDA peaking at 2.35 eV, correlating with the H centre absorption band, but no other MCDA in the spectral region measured.

The results for KI are shown in figure 9(*b*) in comparison to the total MCDA (figure 9(*a*)). As in KBr, besides the UV transition at 3.1 eV there is another MCDA spectrum at 2.1 eV for V_K centres and the IR bands at 1.55 eV and 1.1 eV have different signs for 90° and 45° oriented V_K centres. H centres show just one band for the perpendicular centres at 2.2 eV.

In table 1 all detected optical and MCDA transitions are summarized.

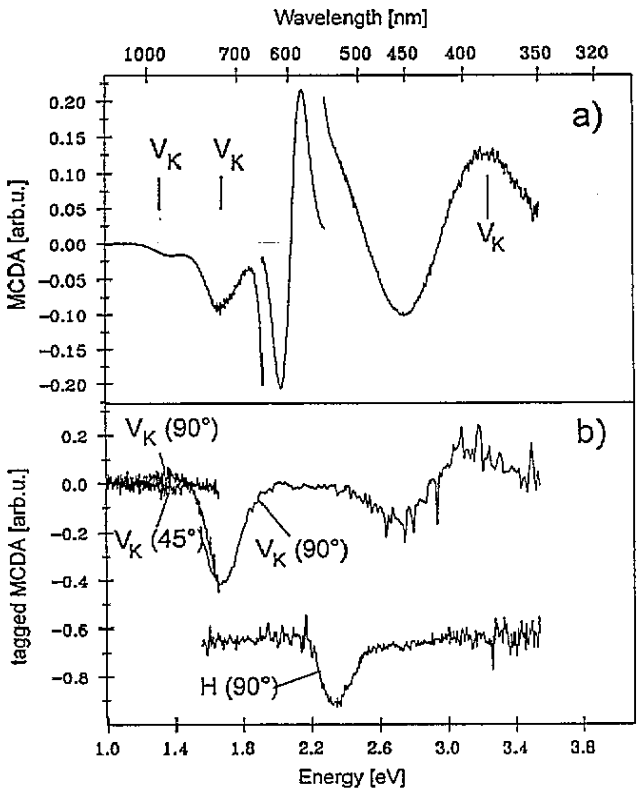

Figure 8. (*a*) MCDA spectra of KBr x-irradiated at 4.2 K *in situ*, measured at $T = 1.5$ K, $B = 2$ T. (*b*) tagged MCDA spectra of V_K and H centres in KBr x-irradiated at 4.2 K, $B_0 \parallel [100]$. The angles in brackets give the orientation of the centre axes with respect to the magnetic field orientation.

4. Discussion

4.1. The simple model of the X_2^- molecular ion

The experimental results obtained for V_K centres in KBr and KI have two unexpected features. One is the additional UV MCDA band at a somewhat lower energy than the known UV absorption band. No absorption bands had yet been reported where we found the MCDA extremum in KBr. However, Delbecq *et al* (1961) have reported an unexpected absorption band at 2.12 eV in KI. The other unexpected feature is the observation that no EPR spectra for parallel centres could be observed with optical detection via the MCDA, neither for the V_K nor for the H centres. For the latter only spectra of perpendicular centres were observed, while for the V_K centres also centres with 45° and 60° orientations could also be seen.

Figure 10 shows the simple molecular ion scheme 'X_2^-' (Schoemaker 1973), which was used for both V_K and H centres to discuss the optical and EPR properties. The UV transition is interpreted as occurring between the $^2\Sigma_u^+ \rightarrow {}^2\Sigma_g^+$ linear combination of halogen valence p orbitals ($^2B_{1u} \rightarrow {}^2A_g$ in the proper D_{2h} symmetry, transition E_σ in figure 10). An external static magnetic field will cause a Zeeman splitting of the Kramers doublets, but for right and left circular polarized transitions the probabilities are equal, so no MCDA effect is expected in the UV in contrast to our observations. The other two allowed dipole transitions

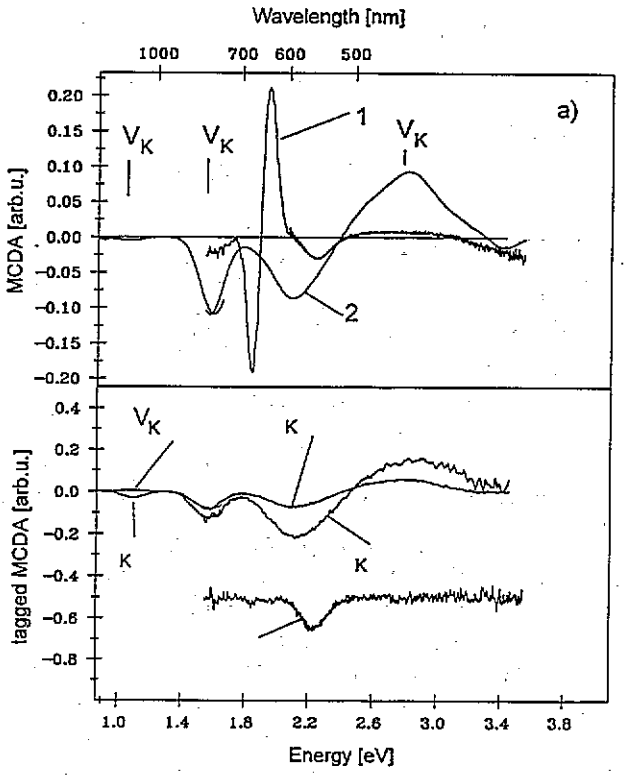

Figure 9. (*a*) MCDA spectra of KI x-irradiated at 4.2 K *in situ*, measured at $T = 1.5$ K, $B = 2$T: curve 1, pure KI; curve 2, Tl-doped KI (doping level 0.5 mol% in the melt). (*b*) Tagged MCDA spectra of V_K and H centres in KI, $B_0 \parallel [100]$. The angles in brackets give the orientations of the centre axes with respect to the magnetic field orientation.

Table 1. Experimental optical absorption bands and MCDA extrema of V_K and H centres in KBr and KI and their assignments to transitions within the X_2^- molecular model.

KBr	V_K	Absorption	*E* (eV)	1.38	1.65	—	3.22	Delbecq *et al*
			Transition	$^2\Sigma_u \rightarrow {}^2\Pi_{g3/2}$	$^2\Sigma_u \rightarrow {}^2\Pi_{g1/2}$	—	$^2\Sigma_u \rightarrow {}^2\Sigma_g$	(1961)
		MCDA	*E* (eV)	1.4	1.65	2.7	3.2	—
	H	Absorption	*E* (eV)	—	2.50	—	3.26	Faraday and Compton (1965)
		MCDA	*E* (eV)	—	2.35	—	—	—
KI	V_K	absorption	*E* (eV)	1.08	1.55	2.12	3.10	Delbecq
			Transition	$^2\Sigma_u \rightarrow {}^2\Pi_{g3/2}$	$^2\Sigma_u \rightarrow {}^2\Pi_{g1/2}$	$^2\Sigma_u \rightarrow {}^2\Pi_u$	$^2\Sigma_u \rightarrow {}^2\Sigma_g$	*et al* (1961)
		MCDA	*E* (eV)	1.1	1.55	2.1	2.8	—
	H	Absorption	*E* (eV)	—	2.23	—	2.78	Konitzer and Hersh (1966)
		MCDA	*E* (eV)	—	2.23	—	—	—

$^2B_{1u} \rightarrow {}^2B_{2g}$, $^2B_{3g}$, (E_π in figure 10) are the IR transitions. These are in fact σ polarized due to the strong spin–orbit coupling and we can expect MCDA bands.

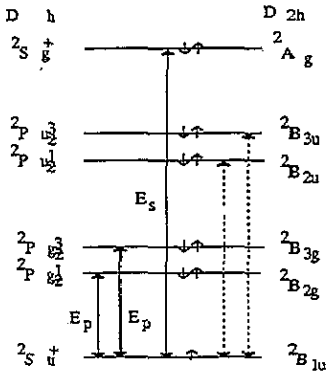

Figure 10. Energy-level scheme for the X_2^- molecule in $D_{\infty h}$ and D_{2h} symmetries. The arrows indicate the dipole-allowed optical π and σ transitions. The dashed arrows indicate dipole-forbidden transitions.

The problem is to explain why we have seen an MCDA in the UV and why we do not see the EPR of parallel centres.

4.2. Analysis of the MCDA transitions of V_K and H centres

We first consider the V_K centres. In the following we derive the MCDA signals in several geometries of the centres relative to the crystal and the applied magnetic field. As explained in the end, it is sufficient to discuss the case of the UV band $^2B_{1u} \rightarrow {}^2Ag$ ($^2\Sigma_u^+ \rightarrow {}^2\Sigma_g^+$). In order to describe how the two molecular orbitals (MOs) mix with other MOs through the spin–orbit coupling and magnetic field, we have to present the symmetry of the even (g) and odd (u) MOs using the basis functions appropriate to the point group D_{2h}. We will use the notation for the free X_2^- molecule below in order to facilitate to see which orbitals mix.

$$\text{u-parity} \qquad |\Sigma_u\rangle : |z\rangle;\ |\Pi_{u1/2}\rangle : |x\rangle;\ |\Pi_{u3/2}\rangle : |y\rangle \tag{1}$$

$$\text{g-parity} \qquad |\Sigma_g\rangle : |s\rangle;\ |\Pi_{g1/2}\rangle : |xz\rangle;\ |\Pi_{g3/2}\rangle : |yz\rangle. \tag{2}$$

Using this basis multiplied with the spin states α and β, the Hamiltonian matrix for the odd-parity portion was given by Fowler *et al* (1973) in their analysis of the self-trapped exciton (STE) luminescence.

The wave functions of the initial state $|\Sigma_u\rangle$ and the final state $|\Sigma_g\rangle$ are obtained from perturbation theory using the matrix of table 2 of Fowler *et al* (1973). Note that table 2 of Fowler *et al* presents matrix elements related to odd-parity MOs. A similar matrix relating to the even-parity MOs using the basis functions given in (1) and (2) can be obtained in an analagous way. It is through the spin–orbit coupling and magnetic field that the original pure states $|\Sigma_u\rangle$ and $|\Sigma_g\rangle$ acquire components of other symmetries, giving rise to possible MCDA transitions.

For two sets of geometries involving the orientation of the centre, direction of $\boldsymbol{B}$ and direction of the light propagation $\boldsymbol{k}$, we can evaluate the dipole matrix elements for the left and right circularly polarized lights. Equations (1) and (2) refer to a coordinate system x, y, z centred on the defect, z being the molecular axis. In order to derive theoretical expressions for the MCDA transition probabilities we have to refer the laboratory frame X, Y, Z, in which the magnetic field orientation is defined (and which is equal to the crystal axis system), to the defect coordinate system. Two specific examples are given below.

(i) V_K centre axis $\parallel \boldsymbol{B} \parallel \boldsymbol{k}$. The V_K centre is aligned along $[1\bar{1}0]$ and $\boldsymbol{B}$ and $\boldsymbol{k}$ are also in the same direction, as shown in figure 11. The external magnetic field $\boldsymbol{B}$ is first expressed in the local coordinate system. Given that field direction of $\boldsymbol{B}$ to be $(0, 0, B)$

in the defect coordinate system, the wave functions $|\Sigma_u\rangle$ and $|\Sigma_g\rangle$, considering the mixing effect of spin–orbit interaction and magnetic field, are

$$|\Sigma_u;\alpha\rangle = |z;\alpha\rangle + a_1|x;\beta\rangle + a_2|y;\beta\rangle \tag{3}$$

$$|\Sigma_g;\alpha\rangle = |s;\alpha\rangle + b_1|xz;\beta\rangle + b_2|yz;\beta\rangle. \tag{4}$$

The coefficients a_1, a_2 and b_1, b_2 represent the mixing coefficients due to spin–orbit coupling for Σ_u and Σ_g, respectively.

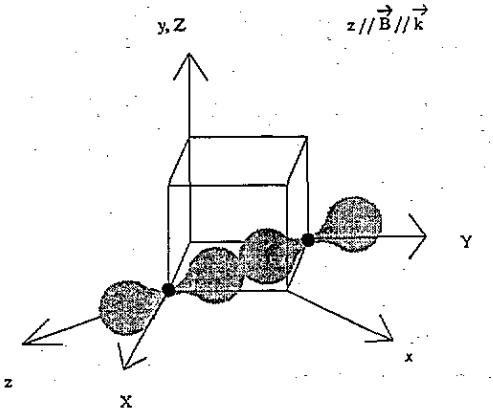

Figure 11. Centre (x, y, z) and laboratory (X, Y, Z) coordinate systems for the case of parallel V_K centres (see text).

The dipole moments for right and left polarized absorption are given by

$$\langle\Sigma_g|\frac{1}{\sqrt{2}}(X+Y) \pm iZ|\Sigma_u\rangle = \langle\Sigma_g|x \pm iy|\Sigma_u\rangle. \tag{5}$$

The evaluation of the above involves the following types of matrix elements, which can be shown to vanish by virtue of symmetry:

$$\langle z;\alpha|x \pm iy|s;\alpha\rangle = 0 \qquad \langle z;\alpha|x \pm iy|xz(yz);\beta\rangle = 0 \tag{6}$$

$$\langle s;\alpha|x \pm iy|x(y);\beta\rangle = 0 \qquad \langle x;\beta|x \pm iy|xz(yz);\beta\rangle = 0. \tag{7}$$

This leads to confirmation that the MCDA of V_K centres in this geometry is absent.

(ii) V_K centre axis $\perp B \parallel k$. In figure 12 one of the two possible orientations of the defect with the axes perpendicular to B is shown (molecular axis $\parallel$ [110] orientation in the laboratory frame). B is parallel to the laboratory [001] axis. The other possible orientation has a V_K centre axis along a $[1\bar{1}0]$ orientation in the laboratory frame. The two contribute to the MCDA and from symmetry it is seen that only one needs analysis. In terms of the defect frame of reference, B is along $(0, B, 0)$ and this is used in expressing Σ_u and Σ_g:

$$|\Sigma_u;\alpha\rangle = (|z;\alpha\rangle - i|z;\beta\rangle) + A_1|x;\alpha\rangle + a_1|x;\beta\rangle + a_2|y;\beta\rangle \tag{8}$$

$$|\Sigma_g;\alpha\rangle = (|s;\alpha\rangle - i|s;\beta\rangle) + B_1|xz;\alpha\rangle + b_1|xz;\beta\rangle + b_2|yz;\beta\rangle. \tag{9}$$

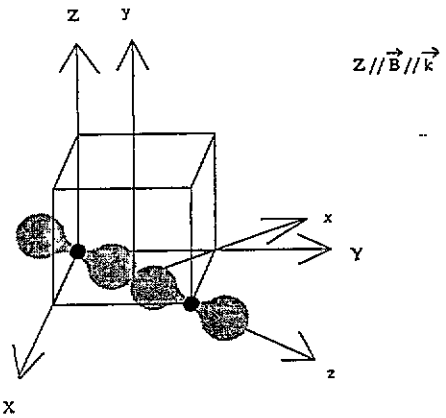

Figure 12. Centre (x, y, z) and laboratory (X, Y, Z) coordinate systems for the case of one of the two possible perpendicular V_K centres (see text).

A_1 and B_1 represent the mixing coefficients due to the magnetic field and they are therefore proportional to the field intensity. For this field direction $|z;\alpha\rangle$ and $|z;\beta\rangle$ are degenerate and, as a consequence, the two vectors have equal weight.

The MCDA matrix elements are

$$\langle\Sigma_g|X \pm iY|\Sigma_u\rangle = \langle\Sigma_g|\tfrac{1}{2}((z-x) \pm i(z+x))|\Sigma_u\rangle. \tag{10}$$

In the evaluation of these matrix elements, one requires several types of integrals. In the following are given those that make non-vanishing contributions:

$$\langle z;\alpha|z|s;\alpha\rangle \qquad \langle z;\beta|x|zx;\beta\rangle \qquad \langle x;\alpha|x|s;\alpha\rangle \qquad \langle x;\beta|z|zx;\beta\rangle. \tag{11}$$

It is somewhat tedious to collect all contributing terms, but it is found that the matrix elements of (11) do not vanish, leading to an observable MCDA signal from those centres that are perpendicular to the magnetic field.

From symmetry arguments, it is seen that those centres in the other perpendicular geometry also make equal contributions to the signal.

The IR band contributes to the MCDA in a similar manner experimentally. This can be explained in the following way. In the IR bands there are the original π components and σ components mixed through spin–orbit coupling. In bromides and iodides the latter component is stronger, so that the IR band overall is σ polarized. In order to discuss the MCDA signal in the parallel and perpendicular geometries, we should consider both the π and σ contributions. The symmetry consideration shows for the parallel centres that there should be a weak but non-zero MCDA signal from the π component to first order. However, for the perpendicular component the contribution to the MCDA is one order of magnitude stronger, being a composite contribution from π and σ components (Meise 1993). The ratio between the parallel and perpendicular MCDA contributions is roughly given by the ratio of π–σ and σ–σ overlaps. It is thought that this explains why we did not observe parallel centres in the IR bands.

We now turn to a brief discussion of the H-centre results. In principle they should also be explainable by the same theoretical model. From the spectral position at the low-energy side of the H centre UV band we assign the MCDA observed for the H centres to the $\Sigma_u \rightarrow \Pi_{g1/2}$ transition. Again, as in the case of the V_K centre, we see only perpendicular centres.

The question remains, why we did not observe an MCDA of perpendicular centres in the UV transition. According to a recent study (Tanimura 1993), the UV bands of the H centre in KBr and NaCl are almost 100% σ polarized. Although the reason for this near perfect polarization (compared to that of the V_K centres) is not understood at present, it is the consequence of near cancellation of the terms leading to the π-polarized component in the UV band of the H centres. The absence of the MCDA in the present case can be attributed to the same circumstances. We note that when calculating the matrix elements for MCDA (10) one finds a large number of non-zero terms with opposite signs (Meise 1993). It may happen that in the case of the H centres there is a cancellation of terms, rendering the MCDA very weak.

4.3. The presence of a new V_K band in the MCDA

The observation of the new V_K band through the MCDA in KBr and KI is now discussed. So far we have considered the $\Sigma_u \rightarrow \Sigma_g$ and the $\Sigma_u \rightarrow \Pi_g$ transitions. There are two more MOs to which the dipole transition is not allowed in the D_{2h} symmetry, the normal geometry of the V_K centre. These are the two Π_u states of different multiplicity (figure 10). These MOs are connected to Σ_u through spin–orbit coupling. Delbecq *et al* (1961) have assigned the band observed at 2.12 eV in KI to a $\Sigma_u \rightarrow \Pi_u$ transition. They argued that the inversion symmetry may be broken by some unspecified distortion. Group theory indicates that when the inversion symmetry is lost $\Sigma_u \rightarrow \Pi_u$ becomes dipole allowed (see e.g. Song and Williams 1993).

Table 1 presents the various absorption bands observed in the present work as well as optically. In the case of KI, the extra band obsrved by Delbecq *et al* (1961) matches well with the data obtained by MCDA. In the case of KBr, there are no available data optically. However, note that at 2.7 eV the optical absorption does not go to zero (figure 1); the V_K band at 3.2 eV seems to have a low-energy tail. It is interesting to note that the presence of the extra band has again never been discussed before. The energy difference for $\Sigma_u \rightarrow \Pi_u$ is generally designated by $E_\perp$ and deduced from the shift of $g_\perp$ with respect to g_e when the spin–orbit coupling parameter is known. The published values of $E_\perp$ for KI and KBr are 2.03 and 2.19 eV, respectively (Schoemaker 1973). These values can be compared with the experimental data 2.1 and 2.7 eV respectively (table 1). The discrepancy can be attributed to the uncertainties of the spin–orbit coupling constant used in the calculation of $g_\perp$.

The H centres on the other hand show generally fewer bands optically and via MCDA. In particular, there is no report of an optical band corresponding to the $\Sigma_u \rightarrow \Pi_u$ transition. We did not observe any bands other than the $\Sigma_u \rightarrow \Pi_{g1/2}$ transition in the present study. It is useful to note here that Känzig and Woodruff (1958) have observed that for the H centres in alkali halides (KCl), Π_u is located above Σ_g in figure 10. If the forbidden transition $\Sigma_u \rightarrow \Pi_u$ should become observable, it should be at the higher-energy side of the UV band.

We now speculate on the possible origin, which may induce a loss of inversion symmetry in the V_K centre. Available calculations (Itoh *et al* 1980) indicate that the axial transitional mode of vibration is the softest local mode of the V_K centre. According to Harding, quoted in Itoh *et al* (1980), in KCl this mode has a frequency of 1.17×10^{12} s^{-1} (4.8 meV). On the other hand, from the analysis of the π band shape as a function of temperature in NaCl, Suzuki *et al* (1989) have deduced a frequency of 1.94×10^{12} s^{-1} (7.9 meV). We propose therefore that the very slow axial oscillations of the centre make the centre seem 'frozen' at the classical turning points during the optical transition. This is equivalent to having a momentarily off-centre geometry, thereby making the $\Sigma_u \rightarrow \Pi_u$ transition allowed. The soft frequency is fast compared to the frequencies of about 10 GHz used in conventional EPR spectroscopy, therefore this symmetry breaking is not seen in conventional EPR. Whether

a similar mechanism may be in operation in H centres is not clear. The axial transitional mode has not been calculated. The H-centre (axial) diffusion activation energy is very small, about 100 meV or less (Song and Williams 1993), and it can be argued that the mode is very soft. A good theoretical evaluation, preferably by an *ab initio* Hartree–Fock method, of these parameters would be interesting.

5. Conclusions

With the MCDA method the absorption bands of V_K and H centres could be identified unambiguously correlating them to their respective EPR spectra. It could furthermore detect dynamical features, which cannot be seen by conventional EPR and were not very clear from optical absorption spectroscopy. From the point of view of practical application of the highly sensitive MCDA-detected EPR for the study of scintillator crystals it is important to know that only certain centre orientations with respect to the magnetic field orientations can be detected.

Acknowledgments

We would like to thank K Tanimura for discussion about the H-centre bands.

References

Cade P E, Stoneham A M and Tasker P W 1984 *Phys. Rev.* B **30** 4621
Delbecq C J, Hayes W and Yuster P H 1961 *Phys. Rev.* **121** 1043
Eachus R S, McDugle W G, Nuttal R H D, Olm M T, Kochnick F K, Hangleiter Th and Spaeth J M 1991a *J. Phys.: Condens. Matter* **3** 9327
—— 1991b *J. Phys.: Condens. Matter* **3** 9339
Faraday B J and Compton W D 1965 *Phys. Rev.* A **138** 893
Fowler W B 1968 *The Physics of Color Centres* ed W B Fowler (New York: Academic) pp 553, 627
Fowler W B, Marrone M J and Kabler M N 1973 *Phys. Rev.* B **8** 5909
Itoh N 1972 *Cryst. Latt. Defects* **3** 115
Itoh N, Stoneham A M and Harker A H 1980 *J. Phys. Soc. Japan* **49** 1364
Känzig W and Woodruff T D 1958 *J. Phys. Chem. Solids* **9** 70
Konitzer J D and Hersh H N 1966 *J. Phys. Chem. Solids* **27** 771
Koschnick F K, Spaeth J M and Eachus R S 1992a *J. Phys.: Condens. Matter* **4** 3015
—— 1992b *J. Phys.: Condens. Matter* **4** 8919
Meise W 1993 *Doctoral Thesis* University of Paderborn
Schoemaker D 1973 *Phys. Rev.* B **7** 786
Song K S and Williams R T 1993 *Self Trapped Excitons (Springer Series in Solid State Sciences 105)* (Berlin: Springer)
Spaeth J M, Meise W, Song K S 1993 *J. Phys.: Condens. Matter* to be submitted
Spaeth J M, Niklas J R and Bartram R H 1992 *Structural Analysis of Point Defects in Solids (Springer Series in Solid State Sciences 43)* (Berlin: Springer) ch 4
Suzuki S, Tanimuira K, Itoh N and Song K S 1989 *J. Phys.: Condens. Matter* **1** 6993
Tanimura K 1993 private communication